DOI: 10.1002/ejic.200600619

Electronic Control of the Rotational Barrier in η^2-Alkyne-1-thio Complexes

Wolfram W. Seidel,*[a] Beatriz López Sánchez,[a] Matthias J. Meel,[a] Alexander Hepp,[a] and Tania Pape[a]

Keywords: (Alkylthio)alkyne ligands / Alkyne complexes / Molybdenum / Fluxionality / Ligand effects

A family of thio-alkyne complexes [Tp′Mo(CO)(L)($BnSC_2S$)] {Bn = benzyl, Tp′ = hydrotris(3,5-dimethylpyrazolyl)borate, L = carbonyl (**2**), 2,6-dimethylphenyl isocyanide (**7**), *tert*-butyl isocyanide (**8**), 4-(dimethylamino)pyridine (**9**)} was prepared by reductive removal of a benzyl group in the corresponding bis(benzylthio)acetylene complexes [Tp′Mo(CO)(L)-($BnSC_2SBn$)](PF_6) (**1**-PF_6, **4**-PF_6, **5**-PF_6 and **6**-PF_6). All complexes were characterized by IR, ^1H, ^{13}C spectroscopy and cyclic voltammetry. X-ray diffraction studies of **5**-PF_6, **8** and **9** were carried out. The alkyne ligand is bound symmetrically to molybdenum in **5**-PF_6 and unsymmetrically in **8** and **9**. The trend in the π-acidity of ligand L is reflected in the spectroscopic and electrochemical data as well as in the molecular structures. Variable temperature ^1H NMR investigations with **7**, **8** and **9** disclosed that the barrier of the alkyne rotation at molybdenum decreases in the order of rising electron density at the metal center while the steric demand increases. Therefore, electronic control of the barrier by the specific character of the ligand L is evident.

Introduction

Applying the terms of simple VB theory alkynes can act in their complexes as two-, three- or four-electron donor ligands. The possible interaction of two occupied π- and two unoccupied π*-alkyne orbitals with metal orbitals renders an appropriate description of the binding situation more complex compared to the Dewar–Chatt–Duncanson model for coordinated alkenes. However, the easy rotation of the side on bound ligand is of typical behaviour for both alkene and alkyne complexes. In asymmetric alkyne complexes this dynamic behaviour can regularly be studied by variable temperature NMR spectroscopy. In this context, the evaluation of both the alkyne-$\pi_\perp$-donation into the metal dπ manifold, and the alkyne-$\pi_\parallel$*-acceptance of metal dπ density seems feasible, because the activation barrier of the rotation should reflect the strength of the metal alkyne π-interaction. The dependence of the rotational barrier from electronic factors such as the π-acid-π-base properties of ancillary ligands[1] and the type of the alkyne[2] is evident in many examples. Electronic factors must be involved, when the observed trend within related complexes does not follow the varying steric demand.[1c] Large barrier differences in complexes with high electronic and steric similarity like [Mo(η^5-C_5H_5)(dppe)(MeC_2Me)](BF_4) and [Mo(η^5-C_5H_5)(PPh_2Me)$_2$(MeC_2Me)](BF_4) emphasize the importance of the particular position of the ligand π-orbitals with respect to the metal dπ manifold.[1b] In contrast, the size of the alkyl substituents R predominantly accounts for barrier differences in [Nb(η^5-$C_5H_4SiMe_3$)(R)$_2$($Me_3SiC_2SiMe_3$)] complexes.[3] However, frequently the differences in the activation enthalpies are small and the interfering steric and electronic factors can not be separated.[4] Thus, neutral Mo^{II} and W^{II} alkyne complexes with the hydrotris(3,5-dimethylpyrazolyl)borate (Tp′) ancillary ligand show distinctively higher barriers[5] compared to those with hydrotris(pyrazolyl)borate. However, the small differences within [TpM(RC_2R')(CO)I] complexes (M = Mo, W) upon variation of R/R′ can be attributed to both steric and electronic reasons.[6] In formal Mo^{VI} complexes with a strong π-donating imido ligand the rotational barrier is even independent of the type of the alkyne.[7] Recently, in paramagnetic complexes [Mo(η^5-C_5H_5){P(OMe)$_3$}$_2$(RC_2R)] temperature-dependent EPR spectroscopy was used to determine much lower barriers of an approximately quarter-turn alkyne oscillation process at the metal.[8] Depending on the particular d^8-metal[9] or type of the ancillary ligand, observation of rotamers with respect to 90° rotation at the metal, that can be considered as the extreme of an "inverted" rotational barrier, emphasizes the delicate balance of steric and electronic influences.[10]

In the course of our studies on the coordination chemistry of sulfur-substituted alkynes[11] we isolated and characterized a number of closely related (R–S)-alkyne complexes, which allow a surprising insight into the problem discussed above. In the complexes [Tp′Mo(CO)(L)(η^2-$BnSC_2S$)], in

[a] Institut für Anorganische und Analytische Chemie, Westfälische Wilhelms-Universität Münster,
Corrensstraße 30/36, 48149 Münster, Germany
Fax: +49-251-8333108
E-mail: seidelww@uni-muenster.de

Supporting information for this article is available on the WWW under http://www.eurjic.org or from the author.

which the ligand L represents either carbonyl, an isocyanide or a pyridine derivative, the electron density at the metal is increased in this order as can be concluded from IR spectroscopic and electrochemical evidence. The variable-temperature ^{1}H NMR spectroscopic investigations of these complexes showed that the free activation enthalpy of the alkyne rotation is notably lowered, while the steric demand of the ligands rises, respectively. Therefore, the electronic determination of the rotational barrier in the complexes [Tp′Mo(CO)(L)(η²-BnSC$_2$S)], described in this contribution, is remarkably obvious.

Results and Discussion

The (BnS)(S)-alkyne complex [Tp′Mo(CO)$_2$(η²-BnSC$_2$S)] (**2**) with a terminal sulfur atom is accessible by a single electron reduction of the corresponding cationic bis(benzylthio)acetylene complex [Tp′Mo(CO)$_2$(η²-BnSC$_2$SBn)](PF$_6$) **1**-PF$_6$ and the subsequent removal of a benzyl radical.[11] The desired substitution of one carbonyl ligand in **2** was preferably performed with **1**-PF$_6$, since the carbonyls are easier to remove in the electron-poorer cation **1**$^+$. Following a procedure described by Templeton,[5] complex **1**-PF$_6$ was transformed into the acetonitrile complex [Tp′Mo(CO)(CH$_3$CN)(η²-BnSC$_2$SBn)](PF$_6$) (**3**-PF$_6$), which served as a convenient starting material for the introduction of other neutral ligands. The substitution of acetonitrile in **3**-PF$_6$ by 2,6-dimethylphenyl isocyanide, *tert*-butyl isocyanide or 4-(dimethylamino)pyridine in boiling dichloromethane (Scheme 1) proceeds very clean, if **3**-PF$_6$ is analytically pure. A facile and fast purification of **3**-PF$_6$, which is unexpectedly stable, is possible by column chromatography using SiO$_2$ as solid phase and dichloromethane as eluent. The products of the substitution according to Scheme 1, [Tp′Mo(CO)(Me$_2$C$_6$H$_3$NC)(η²-BnSC$_2$SBn)](PF$_6$) (**4**-PF$_6$), [Tp′Mo(CO)(Me$_3$CNC)(η²-BnSC$_2$SBn)](PF$_6$) (**5**-PF$_6$) and [Tp′Mo(CO)(Me$_2$NC$_5$H$_4$N)(η²-BnSC$_2$SBn)](PF$_6$) (**6**-PF$_6$), were isolated by crystallization from dichloromethane solutions after layering with diethyl ether.

The preparation of [Tp′Mo(CO)(Me$_2$C$_6$H$_3$NC)(η²-BnSC$_2$S)] (**7**), [Tp′Mo(CO)(Me$_3$CNC)(η²-BnSC$_2$S)] (**8**) and [Tp′Mo(CO)(Me$_2$NC$_5$H$_4$N)(η²-BnSC$_2$S)] (**9**) was achieved by one-electron reduction of **4**-PF$_6$, **5**-PF$_6$ and **6**-PF$_6$ according to Scheme 1. The reduction at –78 °C resulted in all cases in intensely red molybdenum(I) species, which are characterized by low frequencies of the carbonyl and, in the case of **4** and **5**, isocyanide C–N vibrations. A color change to dark green at ambient temperature indicates the formation of the final products by cleavage of a benzyl radical. The dicarbonyl complex **2** is synthesized following the same procedure using **1**-PF$_6$ as starting material.[11] However, the removal of one benzyl group proceeds much faster with improved yields after reduction of **4**-PF$_6$, **5**-PF$_6$ and **6**-PF$_6$. We believe that this benefit can be attributed to both steric and electronic reasons. The higher steric demand of the ligands L compared to CO hamper the formation of undesired by-products, which were shown to involve attack of

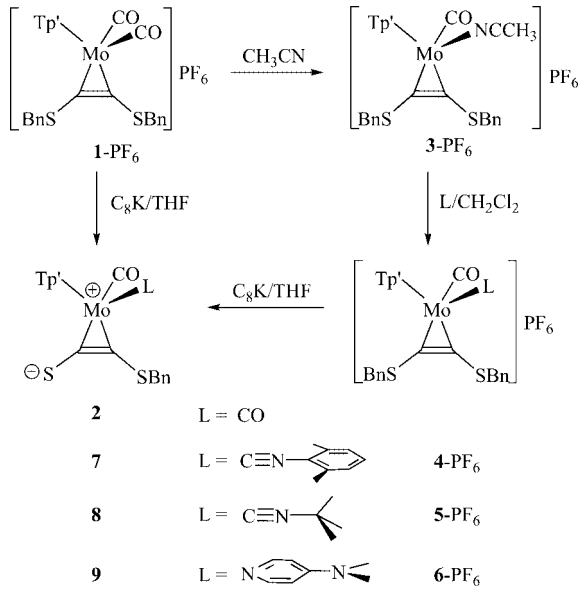

Scheme 1. Synthesis of complexes **2**–**9**, Tp′ = hydrotris(3,5-dimethylpyrazolyl)borate, Bn = benzyl.

benzyl radicals at the coordinated carbonyl.[11] In addition, delocalization of unpaired spin density into the alkyne has been shown to cause the homolytic C–S bond cleavage.[11] Therefore, the facilitated benzyl cleavage in the synthesis of **7**, **8** and **9** compared to that of **2** reflect the higher electron density at the Mo^I species with L. While **7** and **8** can be purified by column chromatography with toluene as eluent, the (dimethylamino)pyridine complex **9** is not sufficiently stable. However, analytically pure **9**·CH$_2$Cl$_2$ was obtained by crystallization from a toluene/CH$_2$Cl$_2$ solution.

The molecular structures of cationic [**5**]$^+$ as well as neutral **8** and **9** (Figure 1 and Figure 2, Table 1) were determined by X-ray structure analysis in order to investigate the steric interference of ligand L with the rotational process of the alkyne ligand. The molecular structures are generally similar and show roughly octahedral polyhedrons considering the alkyne as occupying a single coordination site. The alkyne SCCS planes lie between the two σ-donor-π-acceptor ligands, but rather tilted to the Mo–CO vector to a varying extent. In consideration of the overall similarly complex structures, the removal of one benzyl group ensues one major difference between cationic [**5**]$^+$ and neutral **8** and **9**. While the bis(benzylthio)acetylene ligand is bound symmetrically to molybdenum in [**5**]$^+$, **8** and **9** show one short and one long molybdenum–carbon bond. This observation is reflected in the resonance structure **B** with a thioketo group and one metal carbon double bond (Figure 3). In addition, the SCCS alkyne plane in **8** and **9** is more clearly aligned with the remaining carbonyl ligand compared to [**5**]$^+$. The torsion angle C3–Mo–C2–C1 amounts to 11.6° in **8** and 11.9° in **9**. Despite the rather bulky isocyanides used, replacement of one carbonyl in **2** by an isocyanide does not seem to increase the hindrance of alkyne rotation due to the linear nature of the CNR unit and the longer Mo–CNR bond (compare Mo–C4 2.117(4) Å and Mo–C3 1.996(4) Å

in [**5**]$^+$). However, the steric demand in proximity to the alkyne unit clearly increases from **2** to the 4-(dimethylamino)pyridine complex **9**, in which a sp^2-hybridisized nitrogen atom as a part of an aromatic ring serves as donor. In addition, inspection of the molybdenum alkyne–carbon bond lengths reveals that the Mo–C1 bond is significantly shorter in the 4-(dimethylamino)pyridine complex **9** [2.104(4) Å] compared to the dicarbonyl complex **2** [2.143(3) Å].[11] Therefore, taking into account solely geometric factors the highest rotational barrier is expected for **9**.

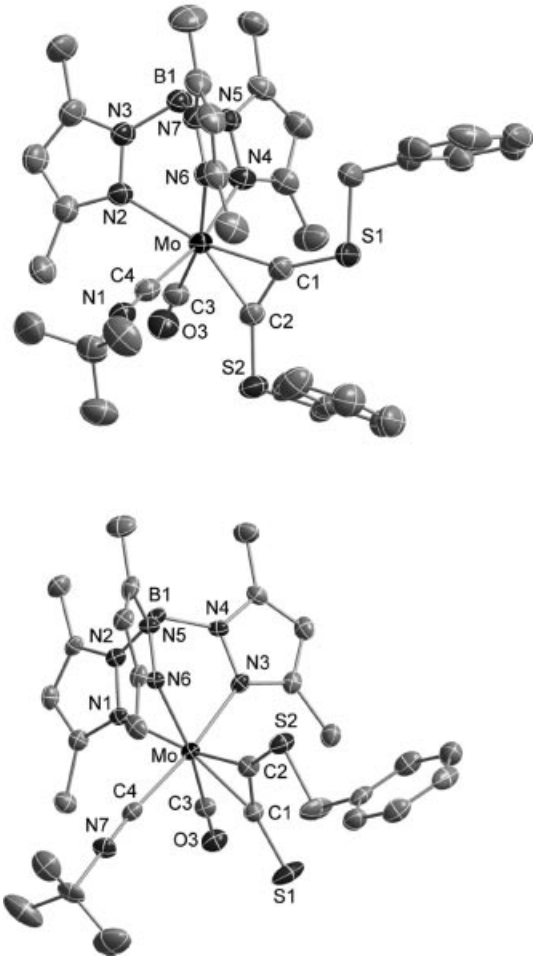

Figure 1. Molecular structures of [**5**]$^+$ (top) and **8** (bottom). Hydrogen atoms have been omitted for clarity.

The increase of the electron density at the molybdenum atom while substituting one carbonyl in **1**-PF_6 with isocyanides in **4**-PF_6 and **5**-PF_6 and 4-(dimethylamino)pyridine in **6**-PF_6 is evident by IR spectroscopy and cyclic voltammetry. Similar observations apply to the series **2**, **7**, **8** and **9**. The prototype complex **1**-PF_6 shows two reversible electron transfer waves at $E_{p,c}$ = –0.80 V and –1.65 V (cathodic peak potentials referenced vs. ferrocene/ferrocenium). The first one at moderate potential is shifted to lower potential, while going to **4**-PF_6 and finally to **6**-PF_6. In turn the CVs. of the more electron rich complexes **4**-PF_6 and **6**-PF_6 show an additional oxidation process (see supporting information). As a result, the second reduction could not even be recorded in the CV of **6**-PF_6. The neutral thio-alkyne complexes **2**, **7** and **8** show concordantly one quasi-reversible electron transfer wave at low potential, while the corresponding reduction process in **9** appears irreversible (Figure 4, Table 2). The cathodic peak potential estimated vs. ferrocene/ferrocenium at a scan rate of 100 mV s^{-1} changes from –1.64 V for **2** to –1.91 V for **7**, –2.01 V for **8** and finally to –2.31 V for **9**. Consistently, in the same order the force constant of the CO stretching vibration decreases from 16.57 N cm^{-1} in **2** to 15.10 N cm^{-1} in **7**, 14.93 N cm^{-1} in **8** and finally to 14.48 N cm^{-1} in **9**. Additionally, the high π-backbonding capacity of molybdenum in **9** is reflected in the hindrance of the pyridine rotation about the Mo–N bond as indicated by ^{1}H NMR spectroscopy.

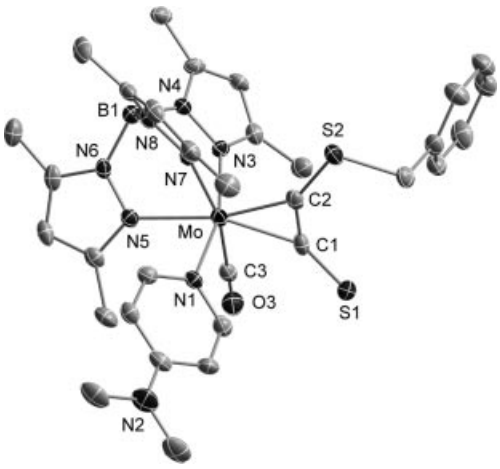

Figure 2. Molecular structure of **9**. Hydrogen atoms have been omitted for clarity.

Table 1. Bonding parameters in thio-alkyne complexes, selected bonds [Å] and angles [°].

	5-PF_6	**8**	**9**
Mo–C1	2.032(4)	2.122(4)	2.104(4)
Mo–C2	2.028(3)	2.006(5)	1.999(4)
Mo–C3	1.996(4)	1.970(4)	1.949(4)
Mo–C4	2.117(4)	2.116(4)	–
Mo–N1	–	–	2.217(3)
C1–C2	1.320(5)	1.345(6)	1.333(6)
C1–S1	1.686(4)	1.659(4)	1.667(4)
C2–S2	1.692(4)	1.700(5)	1.699(4)
C1–C2–S2	145.5(3)	136.2(4)	139.0(4)
C2–C1–S1	137.2(3)	143.8(4)	144.1(4)

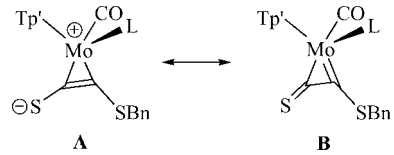

Figure 3. Resonance forms of thio-alkyne complexes.

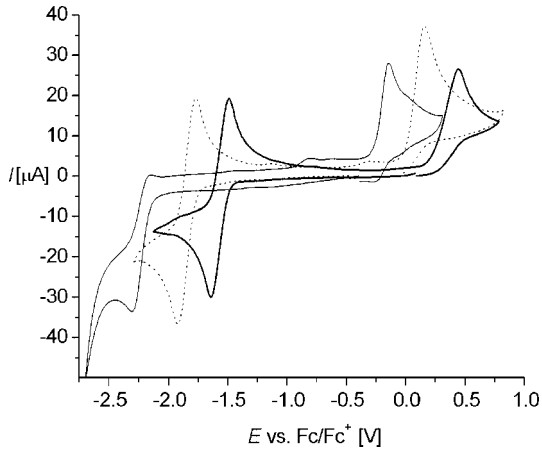

Figure 4. Cyclic voltammograms of **2** (bold line), **7** (dotted) and **9** (line) in CH_2Cl_2.

Table 2. CO force constants, cathodic peak potentials and free activation enthalpies.

	k(CO) /N cm^{-1}	$E_{p,c}$ vs. Fc/Fc$^+$ /V	ΔG^*_{298} ($\Delta G^*_{rev\ 298}$) /kJ mol^{-1}
2	16.57	–1.64	60.5
7	15.10	–1.91	53.1 (51.6)
8	14.93	–2.01	51.5 (51.3)
9	14.48	–2.31	45.5 (42.2)

The room temperature ^{1}H NMR spectra of **2** and **7**–**9** show fluxional behavior, which is particularly evident for the benzylic protons. The alkyne resonances in the ^{13}C NMR spectra of **7** and **8** are in coalescence at ambient temperature. However, at 220 K a double set of signals with one carbonyl and two alkyne resonances for each isomer are found between δ = 220 and 250 ppm. Complex **9** is in fast exchange in the room temperature ^{13}C NMR spectrum and three resonances at 227, 233 and 238 ppm are observed. These values are typical for four-electron donor alkyne complexes.[1a] The underlying dynamic behavior can be attributed to rotation of the unsymmetric thio-alkyne ligand at the metal center based on the following reasons. Alkyne rotation in complexes **2** and **7**–**9** implies an isomer interconversion and both rotamers for **2** and **7**–**9** were observed in the low temperature NMR spectra. The ^{1}H NMR shifts of the benzylic CH_2 protons show a considerable difference of 2 ppm between the two isomers. The similarity of these chemical shifts to the shifts of the two benzyl groups in the cationic bis(benzylthio)acetylene complexes were considered a first hint that alkyne rotation accounts for the fluxional behavior. The resonances of the benzylic CH_2 groups in either *syn* or *anti* position to the carbonyl differ so much because of opposing anisotropy effects by the pyrazole rings and the triple bonds of carbonyl and isocyanide. Therefore, the low field shifted signal is assigned to the *syn* position with respect to the carbonyl ligand, while the high field shifted signal reflects the proximity of the CH_2 group to the pyrazolyl pocket. This perception is proven by 2D NMR spectroscopic experiments.

A gHMBC spectrum of **2** in the slow exchange at 210 K shows the correlation of the PhCH_2 resonance pair with the low field shifted alkyne carbon pair.[11] Accordingly, the gHMBC spectrum of **9** at 300 K in the fast exchange displays correlation of only one of the alkyne carbon atoms with the PhC*H*H resonances (Figure 5). These observations rule out a migration process of the benzyl group from one sulfur atom to the other as reason for the fluxionality because the benzylthio group remains attached to one of the alkyne carbon atoms. In addition, the protons in both isomers of **7**, **8** and **9** are diastereotopic because of the C_1 symmetry of the whole complex. The stereochemistry of the PhC*H*H group is generally retained in the fast exchange, which is evident in the spectrum of **9** at 300 K (Figure 6) and of **8** at 335 K (Figure S7). The difference between the high temperature signal of **9** in $CDCl_3$ (Figure 6) and in CD_2Cl_2 (Figure S9) indicates that the observation of a singlet in the latter case is coincidental. The identity of the isomers, which are not observed in the crystal structures, as *syn* isomer with respect to the benzyl group and the carbonyl ligand, and not as rotamer with respect to the C_{sp}–S bond, is confirmed by a low-temperature ROESY spectrum of **8**. At 210 K both isomers of **8** show proximity of one of the benzyl-CH*H* protons with one of the Tp′ methyl groups, while no correlation to the pyrazol-CH protons was found. In contrast, a weak correlation peak of one benzyl-CH*H* proton of the major isomer with the methyl groups of the isocyanide ligand was detected (see supporting information for details).[12] In addition, DFT calculations were performed in order to estimate the energy differences between four different isomers of the slightly reduced model complex [TpMo(CO)$_2$(MeSC$_2$S)]. Geometry optimizations resulted that the energy differences between the rotational isomers with respect to the C_{sp}–S bond are smaller (approximately 5 kJ/mol) compared to the differences between the isomers with respect to the alkyne rotation at the metal (approximately 10 kJ/mol, see supporting information for details). Finally, the observation of comparable rotational barriers in K[Tp′W(CO)$_2$(η^2-C$_2$S$_2$)] and its complexes without any benzyl group strongly supports our isomer assignment.[13]

While the isomer ratio is largely balanced in **2**, the isomer with the benzyl group directed at the carbonyl is found at the low temperature limit in proportion of 64% in **7**, of 60% in **8** and of 83% in **9**. The primary crystallization of the minor isomers could be attributed to lower solubilities and crystal packing forces. Variable temperature ^{1}H NMR spectra were measured with **7**, **8** and **9** (Figure 6). The coalescence temperature is about ambient temperature for complex **7** and **8**, while the very fast exchange area is out of range. In contrast, the rotational barrier in **9** is so low that the coalescence temperature is just reached at 220 K, while the exchange is fast at room temperature. The activation parameters of **7**–**9** were estimated by line-shape simulation performed with the MEXICO program package[14] (see supporting information for details). The corresponding values of **2** have already been published.[11] The activation parameters obtained are listed in Table 2. The differences are substantial in consideration of the fact that the complexes are very similar and that only one σ-donor/π-ac-

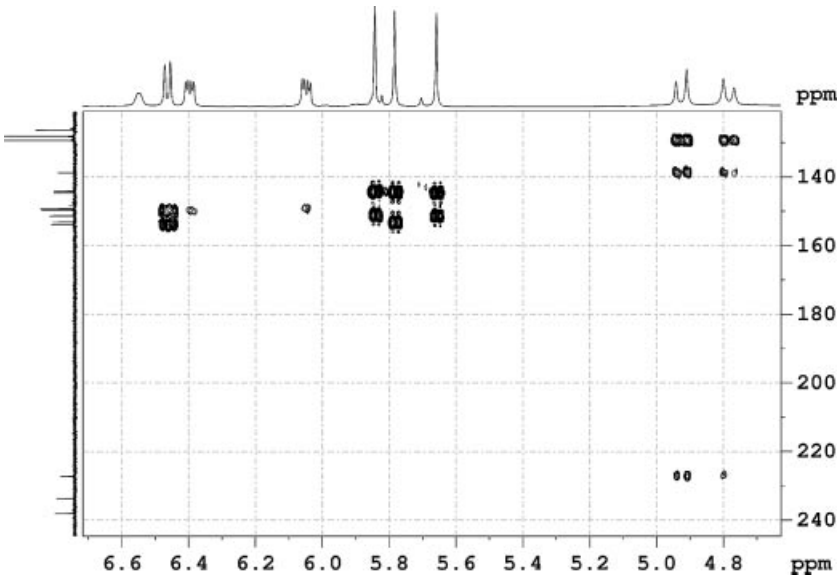

Figure 5. Part of the gHMBC spectrum of **9** at 300 K.

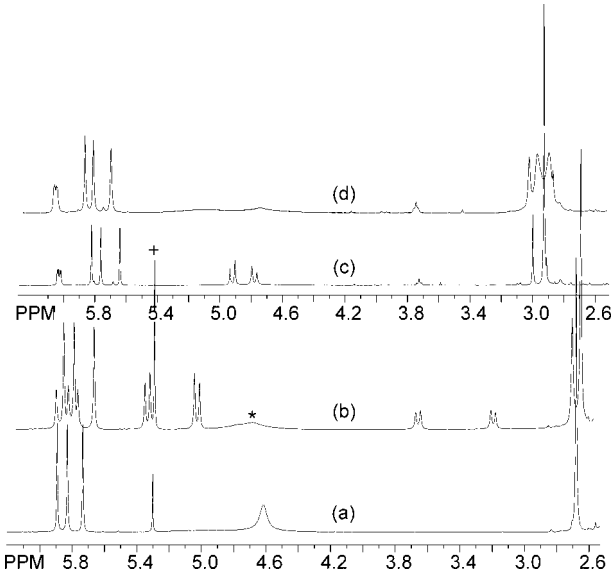

Figure 6. Variable-temperature ^{1}H-NMR spectra in $CDCl_3$: **7** at 335 K (a), **7** at 220 K (b), **9** at 300 K (c) and **9** at 220 K (d), + CH_2Cl_2, * B*H*.

ceptor ligand is varied. The barrier decreases clearly with rising electron density at molybdenum despite increasing steric demand. Therefore the rate of the alkyne rotation must be determined electronically in complexes **2** and **7**–**9** and a crucial contribution of steric factors can be ruled out.

The facilitated rotation of the alkyne with increasing electron density at the metal is not easy to explain, because a stronger back-donation from the metal generally strengthens the π interaction, which is associated with a higher rotational barrier. However, according to a qualitative molecular orbital Scheme for octahedral alkyne d^4-metal complexes presented by Templeton[15,5] two of the frontier orbitals involve metal alkyne π interactions. The bonding combination of the d_{yz} orbital and the $\pi^*_{\|}$ orbital, which represents the π back-donation from the metal, is considered occupied (Figure 7). In contrast, the antibonding combination of the d_{xy} orbital with the $\pi_\perp$-orbital of the alkyne is accounted the LUMO. Templeton has pointed out[1a] that both $\pi_\perp$ and $\pi^*_{\|}$ interchange their partners on the metal, if the alkyne rotates away from the ground state orientation to the orthogonal position with respect to the CO ligand. The π-acidity of the ligand L is particularly important for the d_{xy} orbital, which is considered populated in the excited rotational state.[1a] The perception that ligand L and the alkyne compete for the electron density of the d_{xy} orbital in the excited rotational state reflects the strong influence of the ligand L on the barrier. The decreasing π-acceptor ability in the order CO, isocyanide and pyridine ensues an enhanced π-back bonding to the thio-alkyne ligand resulting in a stabilization of this state. Therefore, the decrease of the rotational barrier can predominantly be attributed to a stabilization of the excited rotational state. In addition, this interpretation explains the otherwise paradox trend of shorter metal–C(alkyne) bonds in the ground-state structure and a facilitated rotation of the alkyne in solution.

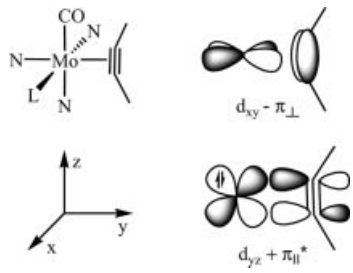

Figure 7. Qualitative molecular orbital Scheme of molybdenum–alkyne π interactions.

Conclusions

Alkyne complexes with a terminal sulfur atom attached to the alkyne are accessible at the Tp′Mo(CO)(L) fragment by reductive cleavage of one benzyl group in the corresponding bis(benzylthio)acetylene complexes [Tp′Mo(CO)(L)(BnSC$_2$SBn)](PF$_6$). The resulting thio-alkyne complexes [Tp′Mo(CO)(L)(BnSC$_2$S)] are interesting as neutral sulfur ligands[16] and as starting materials for the preparation of η²-*C*,*C*′ complexes with acetylenedithiolate.[13] The variation of L with respect to a modified σ-donor-π-acceptor character leads to altered reaction rates in the benzyl cleavage and pronounced trends in the molecular structures, the electrochemical parameters and the solution dynamics. Decreasing π-acidity of L leads to a facilitated rotation of the alkyne at molybdenum. These observations substantiate our strategy to adjust the donor ability on the sulfur atoms in heterobimetallic complexes by slight variations in the coordination sphere of the alkyne complex moiety.

Experimental Section

General Procedures: All operations were carried out under a dry argon atmosphere using standard Schlenk and glove box techniques. All solvents were dried and saturated with argon by standard methods and freshly distilled prior to use. [Tp′Mo(CO)$_2$(BnSC$_2$SBn)]PF$_6$ (**1**-PF$_6$) {Tp′ = hydrotris(3,5-dimethylpyrazolyl)borate}[11] and C$_8$K[17] were prepared according to literature methods. 2,6-dimethylphenyl isocyanide, *tert*-butyl isocyanide and 4-(dimethylamino)pyridine were purchased from Aldrich. ^{1}H and ^{13}C NMR spectra were recorded on a Bruker AC 200 and Bruker Avance 400 NMR spectrometer. Elemental analyses were performed on a Vario EL III CHNS elemental analyzer. ESI mass spectra were obtained using a QUATTRO LCZ (Waters-Micromass). Infrared spectra were recorded on a Bruker Vektor 22. Cyclic voltammetry data was acquired on a ECO/Metrohm PGSTAT 30 potentiostat using a glassy carbon working electrode, an Ag/0.01 M AgNO$_3$/CH$_3$CN reference electrode, (NBu$_4$)(PF$_6$) as supporting electrolyte and ferrocene as internal standard.

[Tp′Mo(CO)(CH$_3$CN){η²-(BnS)CC(SBn)}](PF$_6$) (3-PF$_6$): A solution of **1**-PF$_6$ (3.02 g, 3.50 mmol) in acetonitrile (50 mL) was heated to reflux. After two days the product was isolated by column chromatography at SiO$_2$ using CH$_2$Cl$_2$ as eluent (2.53 g, 83%). Recrystallization from CH$_2$Cl$_2$/Et$_2$O yielded dark green crystals. MS (ESI in CH$_2$Cl$_2$): *m*/*z* = 734 [M]$^+$ with the expected isotopic pattern. IR (KBr): $\tilde{\nu}_{CN}$ = 2179, $\tilde{\nu}_{CO}$ = 1956 cm^{-1}. ^{1}H NMR (200 MHz, CDCl$_3$, 20 °C): δ = 7.46–7.26 (m, 8 H, Ph-*H*), 6.86 (m, 2 H, Ph-*H*), 6.01 (s, 2 H, Tp′-C*H*), 5.95 (s, 1 H, Tp′-C*H*), 5.00 (d, $^2J_{HH}$ = 12.9 Hz, 1 H, SCH*H*), 4.91 (d, $^2J_{HH}$ = 12.9 Hz, 1 H, SC*H*H), 3.49 (d, $^2J_{HH}$ = 12.0 Hz, 1 H, SCH*H*), 2.80 (d, $^2J_{HH}$ = 12.0 Hz, 1 H, SC*H*H), 2.62 (s, 3 H, Tp′-*Me*), 2.51 (s, 9 H, Tp′-*Me*), 2.44 (s, 3 H, Tp′-*Me*), 2.01 (s, 3 H, Tp′-*Me*), 1.42 ppm (s, 3 H, NCC*H*$_3$). ^{13}C NMR (50 MHz, CDCl$_3$, 20 °C): δ = 230.4 (Mo*C*SCH$_2$), 216.5 (*C*O), 207.6 (Mo*C*SCH$_2$), 152.8, 152.1, 149.9, 146.8, 145.8, 142.9 (Tp′-*C*Me), 134.8, 134.0, 129.2, 128.9, 128.8, 128.7, 128.1, 128.0 (Ph-*C*), 108.2, 107.5, 107.3 (Tp′-*C*H), 43.1, 40.5 (S*C*H$_2$), 15.1, 14.2, 14.0, 12.7, 12.5, 7.0 (Tp′-*C*H$_3$), 3.9 ppm (NC*C*H$_3$).

[Tp′Mo(CO)(CN-C$_6$H$_3$Me$_2$-2,6){η²-(BnS)CC(SBn)}](PF$_6$) (4-PF$_6$): A solution of **3**-PF$_6$ (5 g, 5.7 mmol) in dichloromethane (80 mL) was treated with 2,6-dimethylphenyl isocyanide (0.75 g, 5.72 mmol) and heated under reflux for two days. The solution was cooled to ambient temperature and the formation of **4**-PF$_6$ was checked by IR spectroscopy. The solution was reduced in vacuo to 20 mL and layered with diethyl ether (80 mL). After 24 hours green crystals, which had formed, were collected by removing the mother liquor, washing with diethyl ether and drying in vacuo. Yield: 4.4 g (80%). IR (KBr): $\tilde{\nu}_{CN}$ = 2146, $\tilde{\nu}_{CO}$ = 1971 cm^{-1}. ^{1}H NMR (200 MHz, CDCl$_3$, 20 °C): δ = 7.40–7.25 (m,10 H, Ph-*H*), 7.16 (m, 1 H, Ph-*H*), 6.85 (m, 2 H, Ph-*H*), 6.07 (s, 1 H, Tp′-C*H*), 5.97 (s, 1 H, Tp′-C*H*),5.96 (s, 1 H, Tp′-C*H*), 5.41 (br. s, 1 H, B*H*), 4.86 (d, ^2J = 19 Hz, 1 H, SCH*H*), 4.82 (d, ^2J = 19 Hz, 1 H, SC*H*H), 3.35 (d, ^2J = 12 Hz, 1 H, SCH*H*), 2.29 (d, ^2J = 12 Hz, 1 H, SC*H*H), 2.55 (s, 3 H, Tp′-*Me*), 2.53 (s, 3 H, Tp′-*Me*), 2.51 (s, 3 H, Tp′-*Me*), 2.43 (s, 3 H, Tp′-*Me*), 2.24 (s, 6 H, PhC*H*$_3$), 1.88 (s, 3 H, Tp′-*Me*), 1.52 ppm (s, 3 H, Tp′-*Me*). ^{13}C NMR (200 MHz, CDCl$_3$, 20 °C): δ = 226.2 (Mo*C*SCH$_2$), 221.1 (*C*O), 205.1 (Mo*C*SCH$_2$), 168.9 (Mo*C*N), 152.7, 151.6, 150.1, 147.7, 146.4, 146.3 (Tp′-*C*Me), 134.5, 133.2, 130.6, 129.0, 128.9, 128.9, 128.8, 128.8, 129.7, 128.5, 128.3, 128.2 (Ph-*C*), 108.5, 107.4, 107.3 (Tp′-*C*H), 44.1, 41.4 (S*C*H$_2$), 18.5 (Ph-*C*H$_3$), 15.6, 14.6, 14.0, 13.0, 12.6, 12.5 ppm (Tp′-*C*H$_3$).

[Tp′Mo(CO)(Me$_3$CNC){η²-(BnS)CC(SBn)}](PF$_6$) (5-PF$_6$): The complex was synthesized analogously to **4**-PF$_6$ using **3**-PF$_6$ (2.58 g, 2.95 mmol) and *tert*-butyl isocyanide (0.34 mL, 2.95 mmol). Recrystallization from CH$_2$Cl$_2$/Et$_2$O yielded green crystals (2.58 g, 76%). MS (ESI in CH$_2$Cl$_2$): *m*/*z* = 776 [M]$^+$ with the expected isotopic pattern. IR (KBr): $\tilde{\nu}_{CN}$ = 2179, $\tilde{\nu}_{CO}$ = 1971 cm^{-1}. ^{1}H NMR (200 MHz, CDCl$_3$, 20 °C): δ = 7.37–7.26 (m, 8 H, Ph-*H*), 6.89 (m, 2 H, Ph-*H*), 6.05 (s, 1 H, Tp′-C*H*), 5.99 (s, 1 H, Tp′-C*H*), 5.96 (s, 1 H, Tp′-C*H*), 4.88 (d, $^2J_{HH}$ = 13.5 Hz, 1 H, SCH*H*), 4.75 (d, $^2J_{HH}$ = 13.5 Hz, 1 H, SC*H*H), 3.28 (d, $^2J_{HH}$ = 12.0 Hz, 1 H, SCH*H*), 2.85 (d, $^2J_{HH}$ = 12.0 Hz, 1 H, SC*H*H), 2.63 (s, 3 H, Tp′-*Me*), 2.51 (s, 3 H, Tp′-*Me*), 2.50 (s, 3 H, Tp′-*Me*), 2.41 (s, 3 H, Tp′-*Me*), 1.84 (s, 3 H, Tp′-*Me*), 1.49 [s, 9 H, C(C*H*$_3$)$_3$], 1.48 ppm (s, 3 H, Tp′-*Me*). ^{13}C NMR (100 MHz, CDCl$_3$, 20 °C): δ = 228.4 (Mo*C*SCH$_2$), 219.7 (*C*O), 204.0 (Mo*C*SCH$_2$), 152.8, 151.5, 150.0, 147.7, 146.3 (Tp′-*C*Me, two resonances are accidentally isochronic), 135.2, 133.4, 129.1, 129.0, 128.8, 128.7, 128.4, 128.3 (Ph-*C*), 108.5, 107.4, 107.3 (Tp′-*C*H), 60.0 [*C*(CH$_3$)$_3$], 44.0, 41.0 (S*C*H$_2$), 30.0 [C-(*C*H$_3$)$_3$], 15.6, 14.3, 14.1, 13.0, 12.6, 12.5 ppm (Tp′-*C*H$_3$).

[Tp′Mo(CO)(NC$_5$H$_4$NMe$_2$){η²-(BnS)CC(SBn)}](PF$_6$) (6-PF$_6$): The complex was synthesized analogously to **4**-PF$_6$ using **3**-PF$_6$ (3.24 g, 3.65 mmol) and 4-(dimethylamino)pyridine (668 mg, 5.48 mmol). Recrystallization from CH$_2$Cl$_2$/Et$_2$O yielded dark green crystals (2.75 g, 79%). MS (ESI in CH$_2$Cl$_2$): *m*/*z* = 815 [M]$^+$ with the expected isotopic pattern. IR (KBr): $\tilde{\nu}_{CO}$ = 1937 cm^{-1}. ^{1}H NMR (200 MHz, CDCl$_3$, 20 °C): δ = 8.10 (d, ^3J = 6.1 Hz, 1 H, NC*H*), 7.40–7.26 (m, 8 H, Ph-*H*), 6.83 (m, 2 H, Ph-*H*), 6.40 (d, ^3J = 6.1 Hz, 1 H, NC*H*), 6.30 (m, 1 H, NCHC*H*), 6.25 (m, 1 H, NCHC*H*), 6.04 (s, 1 H, Tp′-C*H*), 5.93 (s, 1 H, Tp′-C*H*), 5.91 (s, 1 H, Tp′-C*H*), 4.98 (d, $^2J_{HH}$ = 12.8 Hz, 1 H, SCH*H*), 4.87 (d, $^2J_{HH}$ = 12.8 Hz, 1 H, SC*H*H), 3.48 (d, $^2J_{HH}$ = 11.7 Hz, 1 H, SCH*H*), 3.06 [s, 6 H, N(C*H*$_3$)$_2$], 2.65 (d, $^2J_{HH}$ = 11.7 Hz, 1 H, SC*H*H), 2.54 (s, 3 H, Tp′-*Me*), 2.48 (s, 3 H, Tp′-*Me*), 2.44 (s, 3 H, Tp′-*Me*), 1.92 (s, 3 H, Tp′-*Me*), 1.55 (s, 3 H, Tp′-*Me*), 1.39 ppm (s, 3 H, Tp′-*Me*). ^{13}C NMR (100 MHz, CDCl$_3$, 20 °C): δ = 233.2 (Mo*C*SCH$_2$), 213.8 (*C*O), 205.4 (Mo*C*SCH$_2$), 154.5, 153.1, 152.6, 150.4, 149.7, 149.2 (Tp′-*C*Me), 146.8 (N*C*H), 146.5 (N*C*H), 146.2 [*C*N(CH$_3$)$_2$], 135.0, 134.4, 129.2, 129.1, 128.9, 128.8, 128.4, 128.1 (Ph-*C*), 108.6 (Tp′-*C*H), 108.3 (NCH*C*H), 108.2, 107.6 (Tp′-*C*H), 106.9

(NCH*C*H), 42.9 (S*C*H$_2$), 40.3 [N(*C*H$_3$)$_2$], 39.6 (S*C*H$_2$), 14.6, 14.4, 13.7, 13.0, 12.9, 12.8 ppm (Tp′-*C*H$_3$).

[Tp′Mo(CO)(CN-C$_6$H$_3$Me$_2$-2,6){η^2-(BnS)CC(S)}] (7): At –78 °C potassium graphite C_8K (583 mg, 4.3 mmol) was added to a solution of **4**-PF_6 (3.5 g, 3.6 mmol) in THF (150 mL) leading to an intense red solution. The mixture was stirred for 12 h at room temperature while the solution turned olive-coloured. The product was isolated by column chromatography at SiO_2 using toluene as eluent (1.2 g, 45%). Evaporation of dichloromethane from a dichloromethane/*n*-hexane solution of **7** yielded dark green crystals. $C_{34}H_{38}BMoN_7OS_2$ (731.59): calcd. C 55.82, H 5.24, N 13.40, S 8.77; found C 55.67, H 5.26, N 13.28, S 8.69. IR (KBr): $\tilde{\nu}_{CN}$ = 2108, $\tilde{\nu}_{CO}$ = 1915 cm^{-1}. ^{1}H NMR (200 MHz, $CDCl_3$, 57 °C): δ = 7.25–7.15 (m, 8 H, Ph-*H*), 5.87 (s, 1 H, Tp′-C*H*), 5.80 (s, 1 H, Tp′-C*H*), 5.71 (s, 1 H, Tp′-C*H*), 4.59 (s, 2 H, SCH$_2$), 2.65 (s, 3 H, Tp′-*Me*), 2.47 (s, 3 H, Tp′-*Me*), 2.42 (s, 3 H, Tp′-*Me*), 2.38 [s, 6 H, C$_6$H$_3$(C*H*$_3$)$_2$], 2.35 (s, 3 H, Tp′-*Me*), 2.03 (s, 3 H, Tp′-*Me*), 1.57 ppm (s, 3 H, Tp′-*Me*). ^{1}H NMR (400 MHz, $CDCl_3$, –63 °C): δ = 5.25 (d, ^2J = 12.1 Hz, 64% 1 H, C*H*H), 5.13 (d, ^2J = 12.1 Hz, 64% 1 H, CH*H*), 3.55 (d, ^2J = 11.4 Hz, 36% 1 H, C*H*H), 3.09 (d, ^2J = 11.4 Hz, 36% 1 H, CH*H*). ^{13}C NMR (50 MHz, $CDCl_3$, 20 °C): δ = 232.2, 231.1 (Mo*C*S, Mo*C*O), 179.9 (*C*N), 153.3, 151.4, 151.0, 145.3, 144.4, 144.2 (Tp′-*C*Me), 137.6, 134.3, 129.2, 128.6, 128.3, 127.9, 127.8, 126.8 (Ph-*C*), 107.3, 106.5, 106.5 (Tp′-*C*H), 37.7 (S*C*H$_2$), 19.2 [C$_6$H$_3$(*C*H$_3$)$_2$], 15.5, 15.1, 14.3, 12.9, 12.8, 12.6 ppm (Tp′-*C*H$_3$). ^{13}C NMR (100 MHz, $CDCl_3$, –63 °C): δ = 246.2, 242.1, 232.3, 231.6, 231.2, 231.0 ppm (Mo*C*S, Mo*C*O), other signals have been omitted for clarity.

[Tp′Mo(CO)(Me$_3$CNC){η^2-(BnS)CC(S)}] (8): The complex was synthesized analogously to **7** using **5**-PF_6 (1.14 g, 1.24 mmol) and C_8K (200 mg, 1.48 mmol) in THF (80 mL). Yield after chromatography: 730 mg (86%). Recrystallization from CH_2Cl_2/Et_2O yielded dark green crystals. $C_{30}H_{38}BMoN_7OS_2$ (683.54): calcd. C 52.71, H 5.60, N 14.34, S 9.38; found C 52.56, H 5.76, N 14.18, S 9.21. IR (KBr): $\tilde{\nu}_{CN}$ = 2144, $\tilde{\nu}_{CO}$ = 1922 cm^{-1}. ^{1}H NMR (200 MHz, $CDCl_3$, 20 °C): δ = 7.22 (m, 5 H, Ph-*H*), 5.91 (s, 1 H, Tp′-C*H*), 5.88 (s, 1 H, Tp′-C*H*), 5.75 (s, 1 H, Tp′-C*H*), 2.75 (s, 3 H, Tp′-*Me*), 2.48 (s, 3 H, Tp′-*Me*), 2.44 (s, 3 H, Tp′-*Me*), 2.37 (s, 3 H, Tp′-*Me*), 1.98 (s, 3 H, Tp′-*Me*), 1.55 (s, 3 H, Tp′-*Me*), 1.52 ppm [s, 9 H, C(C*H*$_3$)$_3$]. ^{1}H NMR (400 MHz, $CDCl_3$, –63 °C): δ = 5.25 (d, ^2J = 12.5 Hz, 60% 1 H, C*H*H), 5.12 (d, ^2J = 12.5 Hz, 60% 1 H, CH*H*), 3.55 (d, ^2J = 12.0 Hz, 40% 1 H, C*H*H), 3.09 (d, ^2J = 12.0 Hz, 40% 1 H, CH*H*). ^{13}C NMR (50 MHz, $CDCl_3$, 20 °C): δ = 232.9, 231.3 (Mo*C*S, Mo*C*O), 162.8 (*C*N), 153.1, 151.1, 150.4, 145.2, 144.2, 144.0 (Tp′-*C*Me), 137.6, 129.0, 128.1, 126.6 (*C*$_6$H$_5$), 107.2, 106.3, 106.1 (Tp′-*C*H), 57.5 [*C*(CH$_3$)$_3$], 37.7 (S*C*H$_2$), 30.5 [C(*C*H$_3$)$_3$], 15.2, 14.3, 14.1, 12.7, 12.5, 12.4 ppm (Tp′-*C*H$_3$). ^{13}C NMR (100 MHz, $CDCl_3$, –63 °C): δ = 242.5, 238.0, 232.5, 232.3, 232.2, 231.7 ppm (Mo*C*S, Mo*C*O), other signals have been omitted for clarity.

[Tp′Mo(CO)(NC$_5$H$_4$-4-NMe$_2$){η^2-(BnS)CC(S)}] (9): At –78 °C C_8K (111 mg, 0.82 mmol) was added to a solution of **6**-PF_6 (650 mg, 0.68 mmol) in THF (80 mL) leading to an intense red solution. The mixture was stirred for 18 h at room temperature while the solution turned green. The solution was filtered, subsequently reduced in volume to 10 mL in vacuo and finally layered with diethyl ether (30 mL). The green solid formed was washed with diethyl ether (2 × 10 mL) and dried in vacuo (345 mg, 70%). Recrystallization from dichloromethane/diethyl ether yielded dark green crystals. $C_{33}H_{41}BCl_2MoN_8OS_2$ (807.52): calcd. C 49.08, H 5.12, N 13.88, S 7.49; found C 49.26, H 5.23, N 13.73, S 7.38. IR (KBr): $\tilde{\nu}_{CO}$ = 1893 cm^{-1}. ^{1}H NMR (400 MHz, $CDCl_3$, 20 °C): δ = 8.93 (d, ^3J = 6.8 Hz, 1 H, NC*H*), 7.25–7.10 (m, 5 H, Ph-*H*), 6.45 (d, ^3J = 6.8 Hz, 1 H, NC*H*), 6.38 (dd, ^3J = 6.8 Hz, ^2J = 3.0 Hz, 1 H, NCHC*H*), 6.03 (dd, ^3J = 6.8 Hz, ^2J = 3.0 Hz, 1 H, NCHC*H*), 5.82 (s, 1 H, Tp′-C*H*), 5.76 (s, 1 H, Tp′-C*H*), 5.64 (s, 1 H, Tp′-C*H*), 4.92 (d, $^2J_{HH}$ = 12.8 Hz, 1 H, SCH*H*), 4.78 (d, $^2J_{HH}$ = 12.8 Hz, 1 H, SC*H*H), 2.93 [s, 6 H, N(C*H*$_3$)$_2$], 2.47 (s, 3 H, Tp′-*Me*), 2.37 (s, 3 H, Tp′-*Me*), 2.36 (s, 3 H, Tp′-*Me*), 1.96 (s, 3 H, Tp′-*Me*), 1.52 (s, 3 H, Tp′-*Me*), 1.35 ppm (s, 3 H, Tp′-*Me*). ^{1}H NMR (400 MHz, CD_2Cl_2, –93 °C): δ = 5.26 (d, ^2J = 12.3 Hz, 83% 1 H, C*H*H), 5.03 (d, ^2J = 12.3 Hz, 83% 1 H, CH*H*), 3.57 (broad, 17% 1 H, C*H*H), the forth CH*H* signal is obscured. ^{13}C NMR (100 MHz, $CDCl_3$, 20 °C): δ = 237.9, 233.7 (Mo*C*S, Mo*C*O), 227.2 (Mo*C*SBn), 153.8, 153.1, 151.4, 151.2, 149.8, 149.2 (Tp′-*C*Me), 144.6 (N*C*H), 144.5 (N*C*H), 144.1 [*C*N(CH$_3$)$_2$], 138.7, 129.3, 128.1, 126.4 (Ph-*C*), 107.2 (Tp′-*C*H), 106.8 (NCH*C*H), 106.6 (Tp′-*C*H), 106.5 (NCH*C*H), 106.3 (Tp′-*C*H), 38.9 [N(*C*H$_3$)$_2$], 36.3 (S*C*H$_2$), 15.0, 14.0, 13.8, 12.8, 12.7, 12.6 ppm (Tp′-*C*H$_3$).

Crystal Structure Determination: Single crystals suitable for X-ray analysis were coated in perfluoropolyether oil and mounted on a glass fiber. The intensity data of the complexes were collected on a Bruker AXS Apex system equipped with a rotating anode. The data were measured using either graphite-monochromated Mo-K_a radiation or Cu-K_a radiation monochromated by a Goebel mirror. Data collection, cell refinement, data reduction and integration as well as absorption correction were performed with the Bruker AXS program packages SMART, SAINT and SADABS. Crystal and space group symmetries were determined using the XPREP program. All crystal structures were solved with SHELXS[18] by direct methods and were refined by full-matrix least-square techniques against F_o^2 with SHELXL.[19] All non-hydrogen atoms were refined anisotropically. The hydrogen atoms were included at calculated positions with fixed thermal parameters.

Crystal Data for 5-PF$_6$:[20] $C_{37}H_{45}BF_6MoN_7OPS_2$, M_r = 919.64 g mol^{-1}, dark green prisms, size 0.23 × 0.19 × 0.14 mm^3, monoclinic, space group *P*2(1)/*n*, *a* = 10.695(2), *b* = 21.182(4), *c* = 18.879(4) Å, β = 102.883(4)°, *V* = 4169.1(14) Å^3, *T* = 153 K, *Z* = 4, $\rho_{calcd.}$ = 1.465 g cm^{-1}, μ(Mo-K_a) = 0.519 mm^{-1}, reflections: 40384 collected, 9563 unique, 8034 observed $F_o \geq 2\sigma(F_o)$, $1.47 \leq \Theta \leq 27.50$, R_{int} = 0.0542, 514 parameter, 0 restrains, R_1(obs) = 0.0577, wR_2(obs) = 0.1406, R_1(all) = 0.0696, wR_2(all) = 0.1470, GOF = 1.089, largest difference peak/hole: 1.077/–0.766 eÅ^3.

Crystal Data for 8:[20] $C_{30}H_{38}BMoN_7OS_2$, M_r = 683.54 g mol^{-1}, dark green plates, size 0.17 × 0.09 × 0.03 mm^3, monoclinic, space group *P*2(1), *a* = 8.409(4), *b* = 12.133(6), *c* = 16.017(8) Å, β = 95.369(9)°, *V* = 1626.9(14) Å^3, *T* = 153 K, *Z* = 2, $\rho_{calcd.}$ = 1.395 g cm^{-1}, μ(Mo-K_a) = 0.567 mm^{-1}, reflections: 15710 collected, 7391 unique, 6095 observed $F_o \geq 2\sigma(F_o)$, $1.28 \leq \Theta \leq 27.50$, R_{int} = 0.0539, 388 parameter, 1 restrain, R_1(obs) = 0.0447, wR_2(obs) = 0.0834, R_1(all) = 0.0636, wR_2(all) = 0.0898, GOF = 0.986, largest difference peak/hole: 0.585/–0.567 eÅ^3.

Crystal Data for 9·CH$_2$Cl$_2$:[20] $C_{33}H_{41}BCl_2MoN_8OS_2$, M_r = 807.51 g mol^{-1}, dark green prisms, size 0.14 × 0.11 × 0.07 mm^3, triclinic, space group $P\bar{1}$, *a* = 10.5994(2), *b* = 11.3942(2), *c* = 17.0769(4) Å, α = 100.314(2)°, β = 100.370(2)°, γ = 110.974(1), *V* = 1826.53(6) Å^3, *T* = 110 K, *Z* = 2, $\rho_{calcd.}$ = 1.468 g cm^{-1}, μ(Cu-K_a) = 5.666 mm^{-1}, reflections: 10829 collected, 6111 unique, 4468 observed $F_o \geq 2\sigma(F_o)$, $2.73 \leq \Theta \leq 70.10$, R_{int} = 0.038, 451 parameter, 0 restrains, R_1(obs) = 0.0452, wR_2(obs) = 0.0959, R_1(all) = 0.0625, wR_2(all) = 0.0997, GOF = 0.922, largest difference peak/hole: 1.005/–0.877 eÅ^3.

Calculations: DFT calculations were performed with the Gaussian 03 package using the hybrid functional B3LYP[21] with a

6-311 g(d,p) basis function set for C, H, B, N, O, S and an energy-consistent pseudopotential for Mo from the Stuttgart group.[22]

Supporting Information (see also the footnote on the first page of this article): Cyclic voltammograms of **4**-PF_6, **5**-PF_6, **6**-PF_6, COSY and ROESY spectra of **7** and **8**, geometry optimized structures of isomers of $[TpMo(CO)_2(MeSC_2S)]$, comprehensive variable temperature ^1H and ^{13}C NMR spectroscopic data of **7**, **8** and **9**, Eyring plots for **7**, **8** and **9** obtained by line-shape analysis. This material is available on the www under http://www.eurjic.org or from the author.

Acknowledgments

The Deutsche Forschungsgemeinschaft is gratefully acknowledged for financial support of this work W. W. S. thanks Prof. F. E. Hahn for generous support.

[1] a) J. L. Templeton, *Adv. Organomet. Chem.* **1989**, *29*, 1–100, and references herein; b) S. R. Allen, P. K. Baker, S. G. Barnes, M. Green, L. Trollope, L. Manojlovic-Muir, K. W. Muir, *J. Chem. Soc., Dalton Trans.* **1981**, 873–884; c) P. B. Winston, S. J. N. Burgmayer, T. L. Tonker, J. L. Templeton, *Organometallics* **1986**, *5*, 1707–1715; d) D. J. Wink, N. J. Cooper, *Organometallics* **1991**, *10*, 494–500; e) A. K. Powell, M. J. Went, *J. Chem. Soc., Dalton Trans.* **1992**, 439–445.
[2] P. Oulie, N. Brefuel, L. Vendier, C. Duhayon, M. Etienne, *Organometallics* **2005**, *24*, 4306–4314.
[3] A. Galindo, M. Gómez, P. Gómez-Sal, A. Martín, D. del Río, F. Sánchez, *Organometallics* **2002**, *21*, 293–304.
[4] H. G. Alt, H. E. Engelhardt, *Z. Naturforsch., Teil B* **1985**, *40*, 1134–1138.
[5] S. G. Feng, C. C. Philipp, A. S. Gamble, P. S. White, J. L. Templeton, *Organometallics* **1991**, *10*, 3504–3512.
[6] D. M. Schuster, J. L. Templeton, *Organometallics* **1998**, *17*, 2707–2715.
[7] E. A. Ison, T. M. Cameron, K. A. Abboud, J. M. Boncella, *Organometallics* **2004**, *23*, 4070–4076.
[8] C. J. Adams, N. G. Connelly, P. H. Rieger, *Chem. Commun.* **2001**, 2458–2459.
[9] G. Marinelli, W. E. Streib, J. C. Huffman, K. G. Caulton, M. R. Gagne, J. Takats, M. Dartiguenave, C. Chardon, S. A. Jackson, O. Eisenstein, *Polyhedron* **1990**, *9*, 1867–1881.
[10] a) M. Etienne, P. S. White, J. L. Templeton, *Organometallics* **1991**, *10*, 3801–3803; b) M. D. Curtis, J. Real, D. Kwon, *Organometallics* **1989**, *8*, 1644–1651; c) G. Smith, R. R. Schrock, M. R. Churchill, W. J. Youngs, *Inorg. Chem.* **1981**, *20*, 387–393; d) M. Etienne, B. Donnadieu, R. Mathieu, J. F. Baeza, F. Jalon, A. Otero, M. E. Rodrigo-Blanco, *Organometallics* **1996**, *15*, 4597–4603.
[11] W. W. Seidel, M. D. Ibarra Arias, M. Schaffrath, M. C. Jahnke, A. Hepp, T. Pape, *Inorg. Chem.* **2006**, *45*, 4791–4800.
[12] We are indebted to one of our reviewers for the inspiring objections in order to clarify the questions of isomer identity and interconversion in solution.
[13] W. W. Seidel, M. Schaffrath, T. Pape, *Angew. Chem.* **2005**, *117*, 7976–7979; *Angew. Chem. Int. Ed.* **2005**, *44*, 7798–7800.
[14] A. D. Bain, G. J. Duns, *Can. J. Chem.* **1996**, *74*, 819–824.
[15] J. L. Templeton, J. L. Caldarelli, S. Feng, C. C. Philipp, M. B. Wells, B. E. Woodworth, P. S. White, *J. Organomet. Chem.* **1994**, *478*, 103–110.
[16] W. W. Seidel, M. D. Ibarra Arias, M. Schaffrath, K. Bergander, *Dalton Trans.* **2004**, 2053–2054.
[17] F. A. Cotton, E. A. Hillard, C. A. Murillo, X. Wang, *Inorg. Chem.* **2003**, *42*, 6063–6070.
[18] G. M. Sheldrick, *SHELXS-97: Program for Crystal Structure Solution*, Universität Göttingen, Göttingen, Germany, **1986**–**1997**.
[19] G. M. Sheldrick, *SHELXL-97: Program for Crystal Structure Refinement*, University of Göttingen, Göttingen, Germany, **1997**.
[20] CCDC-612528 (for **5**-PF_6), -612530 (for **8**), and -612531 (for **9**) contain the supplementary crystallographic data for this paper. These data can be obtained free of charge from The Cambridge Crystallographic Data Centre via www.ccdc.cam.ac.uk/data_request/cif.
[21] A. D. Becke, *J. Chem. Phys.* **1993**, *98*, 5648–5652.
[22] D. Andrae, U. Haeussermann, M. Dolg, H. Stoll, H. Preuss, *Theor. Chim. Acta* **1990**, *77*, 123.

Received: June 30, 2006
Published Online: February 2, 2007

